https://doi.org/10.2352/ISSN.2470-1173.2018.07.MWSF-159

Display Image-Barcodes Using Blue/Red Channel Embedding

Karthik Dinesh, Gaurav Sharma; Department of Electrical and Computer Engineering, University of Rochester; Rochester, NY, USA

Abstract

Barcodes and watermarks offer different trade-offs for carrying data through a displayed image. Barcodes offer robust detection and decoding with high data capacity but are visually obtrusive. Watermarks are imperceptible but their detection and decoding is less robust, and they offer lower data capacity. Image-barcodes straddle this trade-off by attempting to reduce perceptual obtrusiveness compared with conventional barcodes, while minimally compromising data robustness. We propose an image-barcode for display applications that is simple, yet novel. The proposed method encodes the data into a monochrome barcode and embeds it into a suitably chosen region in the blue/red channel of a displayed image. The reduced sensitivity of the human visual system to changes in these channels (particularly the blue channel) reduces the perceptual impact of the image barcode compared with conventional black and white barcodes. The data can, however, still be robustly recovered from a typical color image capture of the displayed image-barcode by decoding only the channels with the embedding. We assess visual distortion and robustness of data recovery for the proposed method and experimentally compare against a baseline black and white barcode for two barcode modes representative of potential usage scenarios. Visual distortion for the proposed method is significantly better. Under typical settings, the proposed method introduces a mean S-CIELAB-CIEDE2000 distortion of $\Delta E = 0.39$ for the blue channel embedding and $\Delta E = 0.35$ for the red channel embedding, compared with $\Delta E = 0.59$ for the baseline method. For data recovery, the blue and red channel embeddings using the proposed method match the 100% decoding success rate and synchronization success rate for the baseline method, although, the pre-error-correction observed mean bit error rate of 0.047% (0.08%) for the blue (red) channel embedding is marginally worse than the performance of the baseline method.

Introduction

Machine readable image-based data interfaces [1], such as barcodes and watermarks, have widespread applications due to their ability to connect the analog physical world and digital cyber world [2–9]. Barcodes encode the data in the form of image patterns and offer high data capacity and robust decoding performance, although at the cost of obtrusive visual appearance. Watermarks hide the data in a pre-existing image maintaining the aesthetics and primary functionality of the image. Although the watermarks are visually imperceptible, they offer lower data capacity and less robust detection and decoding. Image-barcodes [10–13] represent yet another class of image-based data interfaces that reside in space of trade-offs between barcodes and watermarks; the aesthetics are improved compared with barcodes with little compromise in the robustness of data communication.

Traditionally image-based data interfaces have been used in print. With increasing prevalence of high resolution displays and ubiquitous availability of mobile devices with high resolution cameras and adequate computational power, image-based data interfaces are also becoming increasingly common in displays. Specific examples include connectivity for advertised content, immediate information access (for instance at transit points), enabling point-of-sale interactions [14, 15], and encoding boarding pass information displayed on smartphones to automate boarding (Aztec codes are common for this application). For several of these applications, visual appearance is minimally important, whereas for others, such as for personalized advertisements embedded within existing video and image content, it is desirable to minimize the perceptual impact. Several alternative image-based data interfaces have been employed for personalized advertisements. Figure 1 shows a frame from a 45 second commercial on a television show by a fashion retailer [16] which debuted the use of conventional black and white barcodes in television ads. In [17], a novel video barcode technology named Vcode, with high data capacity and real time decoding ability, connects a retailer with a customer by permitting users to download the content to their mobile devices. PiCode and ViCode [11, 18] are aesthetically designed

Figure 1: Conventional (black and white) 2D barcode embedded in a video advertisement [16]

picture-embedding barcodes which maintain a trade-off between visual quality of the image and decoding robustness with higher preference for perceptual aesthetics of the image. Color image-barcodes such as ColorCode [19] and Pictorial Image Code [12] have also been proposed for display advertising. Additionally, digital watermarks have been used create multiple hot-spots [20] in advertisement images/videos with each hot-spot connecting the consumer to different products of interests. In these applications, the obtrusiveness of barcodes is often undesirable, whereas watermarks are often not adequately robust. Additionally watermarks face a challenge in adoption because viewers of the content do not realize that additional functionality is available through watermarks unless some additional visual indication is inserted, de-

feating the unobtrusiveness of the watermark.

The evolution of the media-industry is also driving the use of image-based data interfaces in advertisements. Media generates substantial amount of revenues either from the subscription charges from the consumer or from sales of advertisements. Recently over-the-top (OTT) content providers and subscription services, such as Netflix, have emerged as a significant player in the subscription market challenging traditional broadcast media. The OTT content provider services have lower subscription charges and provides advertising free content to the consumer. Although the consumers are watching more television, they are viewing ad-free content with lower subscription charges. Hence, both the subscription revenues and advertisement incomes are drying up for traditional broadcast and cable media. One approach that is attractive for replacing the subscription and advertisement revenues is to change from the existing interruptive model for advertising in broadcast and cable media, to less obtrusive and more targeted personalized advertisements. The increasing availability of computation and Internet connectivity within the ecosystem of set-top boxes and smart televisions enables such targeted advertising, which can further benefit from the interactivity and instantaneity enabled by image-based data interfaces. The use of such options has also become attractive with the introduction of camera apps for both Android [21] and iOS [22, 23] that natively support barcode decoding.

In this paper we propose a robustly decodable display image-barcode that is simple, yet novel. Data encoded as a monochrome barcode is inserted into a suitably selected region of a displayed image within the blue or red channel. The reduced sensitivity of the human visual system to changes in these channels (particularly for the blue channel) reduces the visual obtrusiveness of the barcode compared to black and white barcodes. At the same time, the embedded data can be robustly decoded from captured images of the displayed image-barcode from the channel used for the embedding, with minimal impact of interference from other color channels in the image. Experiments conducted with two different mode settings of quick response (QR) codes, validate the utility the proposed approach. The method based on the proposed approach has significantly lower visual distortion maintaining synchronization and decoding success rates matching those obtained with conventional black and white barcodes and low bit error rates that are only slightly worse.

The paper is organized as follows: The next section details the data embedding and decoding procedure. The assessment methodology and metrics used for evaluating the scheme and comparing it against alternatives are described in the following section. The fourth section outlines the experiments conducted and summarizes the results, and the fifth and final section concludes the paper.

Display image-barcode using blue/red channel embedding

The data embedding and decoding procedures for the proposed method are shown in Fig. 2. These are individually described in the following subsections. Given the predominance of QR codes, we use these in our illustrations of the proposed approach and in our experiments, although the proposed approach can use any conventional monochrome barcode.

Data Embedding

To provide a concrete yet concise description, we describe the embedding process assuming only blue channel embedding. Red (or green) channel embedding can be described in an analogous, immediately apparent, manner. The left half of Fig 2 illustrates the process for embedding a message m in an original color image $I_i^d(x,y), i \in \{R,G,B\}$ to produce our proposed blue channel embedded display image-barcode $\tilde{I}_i^d(x,y), i \in \{R,G,B\}$, where $i \in \{R,G,B\}$ represents red, green, and blue channels and (x,y) denotes pixel co-ordinates. For the purposes of our description, we will assume that the image values in each of the channels are represented in a normalized range between 0 and 1. The message m is first encoded into a monochrome barcode image represented as $I_{BC}^d(x,y)$. As is common in most barcodes used in practice, the process of encoding the message data into the barcode image includes error correction coding to improve the robustness of data recovery. The proposed blue channel embedded display image-barcode is then obtained by inserting the encoded monochrome barcode image into a suitably selected spatial region in the blue channel of the original image. The process can be mathematically represented as

$$\tilde{I}_i^d(x,y) = \begin{cases} \tilde{I}_i^d(x,y) = I_i^d(x,y) & i = R,G \\ \mathbf{1}_{BC}(x,y) I_{BC}^d(x,y) + (1 - \mathbf{1}_{BC}(x,y)) I_B^d(x,y) & i = B \end{cases} \tag{1}$$

where, $\mathbf{1}_{BC}(x,y)$ represents the indicator function of the spatial region where the barcode $I_{BC}^d(x,y)$ is placed, i.e. $\mathbf{1}_{BC}(x,y)$ takes a value of 1 over the subset of pixels BC corresponding to the region where the barcode is inserted (in the blue channel of the color image) and a value of 0 for all other pixels.

When the generated image-barcode is displayed on a typical RGB display, the spatio-spectral distribution of the corresponding displayed image can be modeled as

$$r(x,y;\lambda) = \sum_{i \in \{R,G,B\}} \tilde{I}_i^d(x,y) P_i(\lambda), \tag{2}$$

where $P_i(\lambda), i \in \{R,G,B\}$ are the spectral distribution of the display RGB primaries. We note that often individual channel image values are nonlinearly encoded through "gamma correction". We note that this has no impact on the barcode region in the blue channel, which is a bi-level image taking values 0 or 1.

Data Decoding

To access the functionality provided by the embedded barcode, the displayed image is captured with a camera, typically in a mobile device such as a smartphone or a tablet. The captured image can be modeled as

$$I_k^c(x,y) = \int s_k(\lambda) r(x,y;\lambda) d\lambda, \tag{3}$$

where $I_k^c(x,y)$ represents the image captured by the k^{th} capture channel and $s_k(\lambda)$ represents the spectral sensitivity for the channel, where $k \in \{R,G,B\}$. Substituting (2) in (3), we obtain,

$$I_k^c(x,y) = \sum_{k,i} q_{ki} \tilde{I}_i^d(x,y), \tag{4}$$

where, for $i,k \in \{R,G,B\}$, $q_{ki} = \int s_k(\lambda) P_i(\lambda) d\lambda$ represents contribution that the i^{th} display primary at max intensity (value of 1)

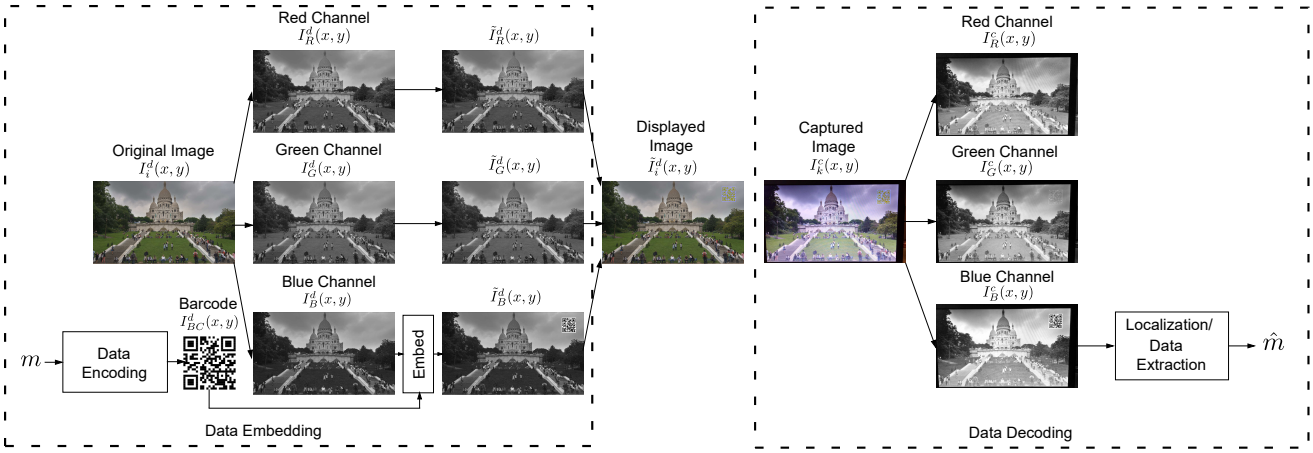

Figure 2: Data embedding and decoding procedure for the proposed blue channel embedded display image-barcode. The individual channel images are represented as grayscale images for clear presentation.

makes to the k^{th} capture channel. The 3×3 matrix $\mathbf{Q} = [q_{ki}]$ models the coupling between the display primaries and the channels in the captured image and the displayed image $\tilde{I}_i^d(x,y)$ spatially modulates the contributions of the primaries from pixel to pixel in order to determine the actual captured image $I_k^c(x,y)$. The diagonal elements in $\mathbf{Q}$ represent the contributions of the R, G, B primaries to the corresponding R, G, B capture channels and the non-diagonal elements represent the cross-talk, or interference, from primaries to non-corresponding capture channels.

In practice, the diagonal elements in $\mathbf{Q}$ dominate the off-diagonal elements. For each of the R, G, and B capture channels the impact of interference from the other display channels is relatively small. Suitable binarization of a channel, invariably eliminates the influence of the interference from other channels and barcode can be localized and decoded from the binarized image. The right half of Fig. 2 illustrates the decoding process for the blue channel embedding scenario. A key advantage of this proposed scheme is that it can advantageously make use of almost all of the existing functionality designed and optimized for the monochrome barcode used for the encoding. In particular, elements used for localization of the barcode and synchronization in the presence of distortions caused by a non-ideal capture geometry, can readily be used in the proposed method. We also note that because the barcode includes localization and synchronization capabilities, we have simplified the notation in the preceding discussion by assuming that the pixel locations (x,y) are identical between the displayed and the captured images.

Assessment Methodology and Metrics

Video advertising represents the primary motivating application for the proposed barcode. Hence, for the data recovery and visual distortion assessments, we utilize a set of 18 keyframes extracted from the Ultra High Definition HEVC DASH Data Set [24] with 1080p (1080×1920) resolution. We consider two modes that we envisage could be used in our proposed application context. In the first mode, which we refer to as the "couch potato" mode, the viewer seeks to capture the information in the displayed image barcode from their normal viewing distance (typically $\approx$ 1.5 times the screen diagonal for televisions). To accommodate capture of the barcode information from the relatively large viewing distances in this mode, the barcode needs to be larger but can flexibly be placed anywhere on the screen. We therefore choose the barcode placement to correspond to a low saliency region in the image and a size that occupies 1.9% of the display area. For the second mode, which we refer to as the "active viewer" mode, the barcode is captured by the viewer after approaching the screen closely, specifically, at a distance of 18 inches in our experiments. For this mode, the barcode is smaller, occupying 0.5% of the display area and placed near the bottom right corner as is typical in current television advertising that uses black and white barcodes. To facilitate synchronization, a uniform border having a value of 1 is additionally included in the channel where the barcode is embedded so as to enlarge each dimension of the barcode by 15%. Figure 3 illustrates the barcode size and placement for these two use scenarios. For both barcode modes, our experiments used a shortened URL as the message m, which was encoded as a version 2 QR code with error correction level L, which nominally corrects upto 7% errors using the Reed-Solomon codes [25] incorporated in the QR code standard. The overall resulting barcode has 25×25 modules.

For evaluating the proposed method we assess both the visual distortion and the data recovery performance and compare these against corresponding metrics computed for a baseline method that uses a black and white barcode (embedded in all the channels of the color image). The baseline method was also tested for the two usage modes with barcode sizes, placements, and capture distances identical to those used for the proposed barcode in the corresponding mode. The only difference between the baseline and the proposed method is that the black and white baseline barcode is embedded in all three channels instead of being confined to the blue or red channel.

For visual distortion assessment, we utilize S-CIELAB [26] in combination with the CIEDE2000 color difference metric [27, 28]. S-CIELAB provides a joint quantitative model for the human visual system's (HVS's) spatio-chromatic sensitivity via a spatial extension of the perceptually uniform CIELAB [29] color space. An S-CIELAB representation corresponding to a color image is obtained in three steps. First a pixel-by-pixel color transfor-

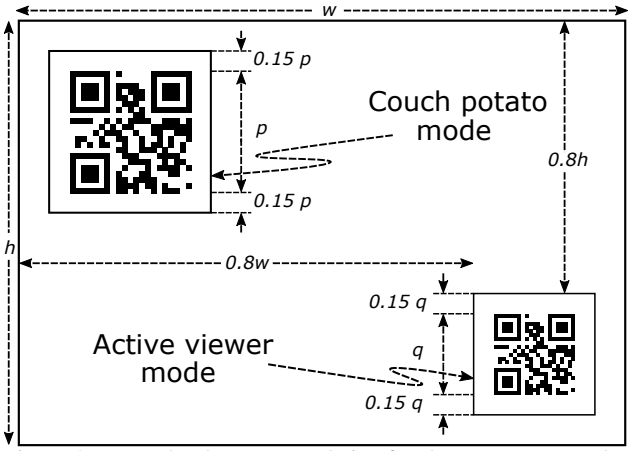

Figure 3: Barcode placement and size for the two usage modes investigated in our experiments. The couch potato mode (top left) uses a larger size barcode that occupies 1.9% of the display area ($p = \sqrt{0.019wh}$) and is placed in a less salient region of the displayed image. The active viewer mode barcode uses a smaller barcode that occupies 0.5% of the display area ($q = \sqrt{0.005wh}$) and is located near the right bottom corner as shown. In both modes, a 15% surrounding border is added to the barcodes as illustrated in the figure. The combination of the barcode and the border defines the region BC of pixels over which the indicator function $I^d_{BC}(x,y)$ in (1) takes a value of 1.

mation is applied to the image to obtain three opponent channel images. Then, based on the varying and approximately independent sensitivity of the HVS to detail in these channels, varying amounts of spatial blur is independently introduced in each of the opponent channel images. Finally, the blurred images are transformed from their opponent color representation into CIELAB on a pixel-by-pixel basis, producing the S-CIELAB representation of the image. Perceived spatio-chromatic differences between two images are quantitatively assessed by computing the difference between their S-CIELAB representations. Because S-CIELAB models the varying sensitivity of the HVS to spatial detail in the opponent channel images and inherits perceptual uniformity of CIELAB, the differences between S-CIELAB representations are more meaningful than naive computation of pixel-wise difference in either RGB or CIELAB representations. To quantify the magnitude of perceived differences between an original image and an image carrying a barcode, we compute the CIEDE2000 color differences between the S-CIELAB representations pixel-by-pixel, to obtain a ΔE error image. Compared with Euclidean distance in CIELAB, CIEDE2000 provides better perceptual uniformity and importantly for our setting, also mitigates specific known problems in CIELAB that make Euclidean distances in the dark blue regions of CIELAB poor correlates for perceived color differences [30]. From the computed ΔE error image, we compute two different averages for the color differences: a direct arithmetic average and a saliency weighted average that additionally weights the ΔE error image by an estimate of the relative saliency at each pixel in computing the average. The overall process is summarized in Fig. 4 for the assessment of the proposed method with the blue channel embedding (other cases are analogous). In addition to the S-CIELAB-CIEDE2000 color differences, we also additionally compute average CIEDE2000 ΔE difference values, with and without saliency weighting.

Parameters of the viewing geometry required for the computation of S-CIELAB representations, were determined by considering two representative display resolution and size configurations and two viewing distances. A typical computer monitor was represented by a 24 inch (diagonal) 92ppi (pixel per inch) display and a typical television screen was represented by a 55 ppi 40 inch display, both having a 1080p resolution matching our test imageset. For each of the displays, 36 inch (3 ft) and 60 inch (5 ft) viewing distances were considered. For each combination of display configurations and the two viewing distances, we perform visual distortion assessment for both barcode modes using the process outlined earlier in this section. The saliency map required for computation of saliency weighted averages is obtained from the original image using the quaternion DCT based method [31].

To numerically quantify data recovery performance, we utilize synchronization success rate (SSR), bit error rate (BER), and decoding success rate (DSR) as evaluation metrics, which are defined as follows. The synchronization success rate (SSR) is the percentage of captured barcodes for which the decoder is able to synchronize successfully, i.e. correctly localize the barcode based on the patterns that mark its position. The bit error rate (BER) is the percentage of bits in error in the bit streams recovered from synchronized barcodes. The BER is computed by comparing the recovered bit stream against the original bit stream embedded in the barcode before any error correction decoding. The third metric, decoding success rate (DSR), is the percentage of captured and synchronized barcodes that decode successfully after error correction. To assess data recovery for the couch potato and active viewer modes, we experiment using a smartphone[1] to capture the image-barcode displayed on a 24 inch 1080p display. The distance of image capture is 18 inches for the active viewer mode and 36 inches for the couch potato mode. The data is recovered from the captured image using the decoding procedure as described in Data Decoding section. The same procedure is employed for the baseline method to recover the message. SSR, BER, and DSR are evaluated and compared for the proposed and baseline methods.

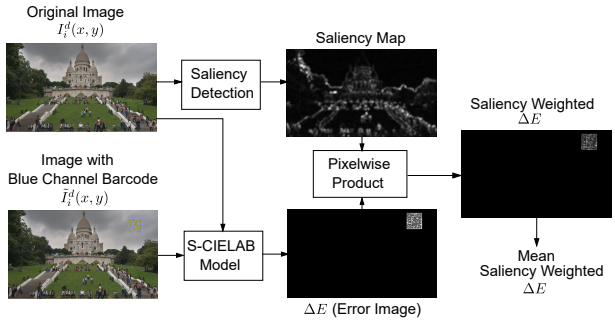

Figure 4: Saliency weighted S-CIELAB-CIEDE2000 error between original image and blue channel image-barcode (proposed method)

Experimental Results

Visual Distortion: As described in third section (Assessment Methodology and Metrics), we assess the visual distortion

[1] Preliminary experiments with additional smartphones provided similar results. An update to include the results obtained with these additional smartphones is pending the completion of the additional experiments.

Barcode Mode	Display Size/ Resolution (in/ppi)	Viewing Distance (in)	Mean ΔE			Mean ΔE	Mean Sal. ΔE			Mean Sal. ΔE
			Proposed			Baseline	Proposed			Baseline
			R	G	B	RGB	R	G	B	RGB
Couch Potato	24/92	36	**1.16**	**2.11**	**1.07**	**2.05**	**0.36**	**0.69**	**0.34**	**0.64**
		60	1.26	2.25	1.16	2.09	0.40	0.75	0.38	0.67
	40/55	36	1.10	2.03	1.02	2.03	0.34	0.65	0.32	0.63
		60	**1.16**	**2.11**	**1.07**	**2.05**	**0.36**	**0.69**	**0.34**	**0.64**
Active Viewer	24/92	36	**0.35**	**0.70**	**0.39**	**0.59**	**0.29**	**0.60**	**0.33**	**0.50**
		60	0.41	0.80	0.47	0.65	0.33	0.69	0.40	0.55
	40/55	36	0.32	0.63	0.35	0.56	0.26	0.54	0.29	0.47
		60	**0.35**	**0.70**	**0.39**	**0.59**	**0.29**	**0.60**	**0.33**	**0.50**

Table 1: Mean and saliency-weighted-mean S-CIELAB-CIEDE2000 ΔE distortion for R, G, and, B channel embeddings for the proposed and baseline methods for the different display configurations, viewing distances, and barcode mode settings. The results in bold highlight typical viewing scenarios where viewing distance is approximately 1.5 times the screen diagonal size.

introduced by our proposed approach and by the baseline method by using the S-CIELAB model and the CIEDE2000 perceptually uniform color difference metric. The mean CIEDE2000 ΔE distortion computed over the barcode regions across all the images in the dataset is approximately 27 (31) and 49, respectively, for the proposed blue (red) channel barcode and the baseline black and white barcode[2]. The average S-CIELAB-CIEDE2000 ΔE distortion is cataloged in Table 1 for the proposed and baseline methods for different embedding channels, different display configurations, viewing distances, and barcode modes averaged over all the test images used in the experiment, where the results corresponding to typical viewing situations are highlighted in bold font. For completeness, the table also includes the distortion values for the case of green channel embedding, which are substantially higher than those for the blue and red channel embedding situations and also slightly larger than those for the baseline. Thus the green channel embedding would normally not be particularly attractive over the baseline and we do not consider it in further experiments[3]. All of the distortion metrics indicate that the proposed approach has a significantly lower visual distortion than the baseline method. Specifically, for typical viewing situations, the proposed method almost halves the distortion over the baseline configuration. Additionally, the metrics also confirm that placing the barcode in regions of low saliency can significantly reduce the perceptual distortion; despite the much larger size of the barcode for the couch potato mode, the saliency weighted errors for the couch potato mode are close to those for the active viewer mode because the larger barcode is placed in low saliency regions.

In Table 1 the proposed method with the blue and red channel embedding options have very comparable distortion values for the corresponding situations. However, our informal visual assessments indicated that the perceived embedding distortion was lower for the blue channel embedding compared with that for the red channel embedding. This discrepancy highlights limitations of the SCIELAB-CIEDE2000 metric. Figure 5 shows some sample frames with the blue and red channel embedding and corresponding baseline along with the computed saliency-weighted-mean S-CIELAB-CIEDE2000 ΔE distortion for these situations. In these figures, it can be appreciated that the embedded barcodes using the proposed approach introduce a relatively small amount of perceptual distortion. Because there is substantial dependence of the distortion on the image content and there can be cases where visually the red channel embedding introduces lower distortion than the blue channel embedding for the same location. The capability for dynamically choosing the channel for embedding can therefore provide an additional avenue for the reduction of visual distortion. In some situations, the perceptual distortion may be further optimized by suitably selecting the embedding channel and co-designing the video content to better mask the distortion over the barcode area. Finally, we note that although we do not consider it because of its poor distortion performance, the proposed methodology could also be used for the green channel. Additionally, the approach also offers the flexibility for using multiple channels. In the specific situation where all three channels are simultaneously utilized for embedding independent payload data, the approach reduces to our previously reported per-channel display color barcodes [32].

Data Recovery: Table 2 summarizes the average SSR, BER, and DSR for the proposed and baseline methods for the couch potato and active viewer modes averaged over the keyframes. For both the couch potato and the active viewer mode and for either choice of blue/red channel embedding, the proposed approach matches the 100% SSR and DSR of the baseline method. For all cases, the BER is quite low and well below the 7% error correction capability of the chosen level of error correction for the QR code used in the experiments. The performance of the baseline method is slightly better than that of the proposed approach. The BER for the proposed blue (red) channel embedding method was 2.52×10^{-3} (1.58×10^{-3}) and 4.7×10^{-5} (8×10^{-5}), respectively, in the couch potato and active viewer modes, whereas no errors were encountered for the baseline method in either mode. The longer capture distance for the couch potato mode results in a higher BER than in the active viewer mode.

The results illustrate that the proposed approach encounters only a small performance degradation in the robustness of data recovery compared with the baseline technique. As already noted, in lieu of this minor loss of data recovery robustness, the method offers a significantly lower visual distortion.

[2] As may be anticipated, the mean CIEDE2000 ΔE distortion over the barcode region is very similar for the couch potato and active viewer modes.

[3] This also justifies the omission of the green channel embedding case from our paper title.

(a) $\Delta E = 0.44$ (b) $\Delta E = 0.18$ (c) $\Delta E = 0.32$

(d) $\Delta E = 0.41$ (e) $\Delta E = 0.35$ (f) $\Delta E = 0.27$

Figure 5: Sample images showing examples of the baseline black and white barcode embedding (leftmost column) and the proposed method with blue channel (middle column) and red channel (rightmost column) embedding. The saliency weighted S-CIELAB-CIEDE2000 ΔE metric for each image are indicated below the image. The top row illustrates an example for which the S-CIELAB-CIEDE2000 ΔE metric is smaller for the blue channel embedding approach compared with the red channel embedding and the bottom row illustrate the converse situation. For the images in both rows, the proposed approach offers a significantly reduction in the visual distortion, which can be appreciated by visual comparison and is also supported by the numerical values.

		Blue channel Embedding			Red Channel Embedding		
Barcode Mode	Method	SSR (%)	BER (%)	DSR (%)	SSR (%)	BER (%)	DSR (%)
Couch Potato	Proposed	100	0.252	100	100	0.158	100
	Baseline	100	0	100	100	0.016	100
Active Viewer	Proposed	100	0.047	100	100	0.080	100
	Baseline	100	0	100	100	0	100

Table 2: Average Synchronization success rate (SSR), Bit error rate (BER), Decoding success rate (DSR) for the proposed and baseline methods for the two different barcode modes for blue/red channel embedding

Conclusion

In this paper, we proposed a simple, yet novel, display image barcode that operates by using the blue/red channel of an image for embedding a barcode. Compared to conventional black and white barcodes, the proposed approach significantly reduces visual distortion, while encountering minimal compromise in data recovery robustness. The proposed methodology is general and can operate with any barcode design, inheriting and exploiting the already optimized design elements from the barcode, such as synchronization and error correction coding. As camera apps in mobile devices become natively enabled for decoding barcodes, the proposed approach offers a particularly attractive option for enabling better interactivity with color displays.

Acknowledgment

This work was supported in part by a distinguished researcher award from the Center of Rochester Center of Excellence in Data Science. We thank the Center for Integrated Research Computing, University of Rochester, for providing access to computational resources.

References

[1] G. Sharma, "Image-based data interfaces revisited: Barcodes and watermarks for the mobile and digital worlds," in *8th Intl. Conf. on Comm. Sys. and Networks (COMSNETS)*, Bangalore, India, Jan. 2016, pp. 1–6.

[2] R. Villn, S. Voloshynovskiy, O. Koval, and T. Pun, "Multilevel 2-D bar codes: toward high-capacity storage modules for multimedia security and management," *IEEE Trans. on Information Forensics and Security*, vol. 1, no. 4, pp. 405–420, 2006.

[3] B. Zhang, K. Ren, G. Xing, X. Fu, and C. Wang, "SBVLC: Secure barcode-based visible light communication for smartphones," *IEEE Trans. on Mobile Computing*, vol. 15, no. 2, pp. 432–446, 2016.

[4] T. Hao, R. Zhou, and G. Xing, "COBRA: color barcode streaming for smartphone systems," in *Procs. of the 10th Intl. Conf. on Mobile Sys., Applications, and Services*. ACM, 2012, pp. 85–98.

[5] O. Bulan, H. Blasinski, and G. Sharma, "Color QR codes: Increased capacity via per-channel data encoding and interference cancellation," in *Proc. IS&T/SID Nineteenth Color and Imaging Conference: Color Science and Engineering Systems, Technologies, and Applications*, San Jose, CA, 7-11 Nov. 2011, pp. 156–159.

[6] A. Reed, E. Rogers, and D. James, "Chrominance watermark for mobile applications," in *Proc. SPIE: Multimedia on Mobile Devices,*, vol. 7542, 2010, pp. 75 420V–1–75 420V–8.

[7] A. Reed, T. Filler, K. Falkenstern, and Y. Bai, "Watermarking spot colors in packaging." in *Proc.SPIE: Media Watermarking, Security, and Forensics*, vol. 9409, 2015, pp. 940 906–940 906.

[8] A. K. Mikkilineni, G. N. Ali, P.-J. Chiang, G. T.-C. Chiu, J. P. Allebach, and E. J. Delp, "Signature-embedding in printed documents for security and forensic applications," in *Proc. SPIE: Security, Steganography, and Watermarking of Multimedia Contents*, vol. 5306, 2004, pp. 455–466.

[9] K. Finlow-Bates and K. Annapureddy, "Embedded barcodes for displaying context relevant information," Oct. 18 2016, US Patent 9,471,824.

[10] O. Bulan, G. Sharma, and B. Oztan, "High capacity image barcodes using color separability," in *Proc. SPIE: Color Imaging XVI: Displaying, Processing, Hardcopy, and Applications*, R. Eschbach, G. G. Marcu, and A. Rizzi, Eds., vol. 7866, Jan. 2011, pp. 7866–N,1–9.

[11] C. Chen, W. Huang, B. Zhou, C. Liu, and W. H. Mow, "PiCode: A new picture-embedding 2D barcode," *IEEE Trans. Image Proc.*, vol. 25, no. 8, pp. 3444–3458, Aug 2016.

[12] C. Cheong, T.-D. Han, J.-Y. Kim, T.-J. Kim, K. Lee, S.-Y. Lee, A. Itoh, Y. Asada, and C. Craney, "Pictorial image code: A color vision-based automatic identification interface for mobile computing environments," in *Eighth IEEE Workshop on Mobile Computing Sys. and Applications, HotMobile 2007.*, 2007, pp. 23–28.

[13] D. L. Hecht, "Embedded data glyph technology for hardcopy digital documents," in *Proc. SPIE: Color hard copy and graphic arts III*, vol. 2171, Feb. 1994, pp. 341–352.

[14] "Wal-mart adds to mobile wallet frenzy with walmart pay." Posted on Dec. 10, 2015 in Reuters.

[15] "Walmart launches mobile payments processor." Posted on Dec. 14, 2015 in Business Insider.

[16] "Bar codes add detail on items in TV ads," Posted on Sept. 27 2010 in The New York Times.

[17] X. Liu, D. Doermann, and H. Li, "VCode-pervasive data transfer using video barcode," *IEEE Trans. Multimedia*, vol. 10, no. 3, pp. 361–371, April 2008.

[18] W. Huang and W. H. Mow, "PiCode: 2D barcode with embedded picture and ViCode: 3D barcode with embedded video," in *Procs. of the 19th Annual Intl. Conf. on Mobile Computing & Networking*. ACM, 2013, pp. 139–142.

[19] H. Tack-don, C. Cheol-ho, L. Nam-kyu, and S. Eun-dong, "Machine readable code image and method of encoding and decoding the same," Mar. 28 2006, US Patent 7,020,327.

[20] "Multiple hot-spots." Posted on Nov. 15 2011 in Digimarc.

[21] "Motorola updates camera and gallery apps, now allows QR code scanning and saving albums to MicroSD." Posted on Aug. 31, 2015 in Tech Times.

[22] "The iPhones camera app can now read QR codes." Posted on Jun. 5, 2017 in TechCrunch.

[23] "Why the "hidden" update in Apple's latest iOS changes the rules of marketing," Posted on Oct. 30, 2017 in Forbes.

[24] J. Le Feuvre, J. Thiesse, M. Parmentier, M. Raulet, and C. Daguet, "Ultra high definition HEVC DASH data set," in *Procs. of 5th ACM Multimedia Sys. Conf.*, 2014, pp. 7–12.

[25] S. Lin and D. J. Costello, Jr., *Error Control Coding*. Englewood Cliffs, NJ: Prentice-Hall, 2004.

[26] X. Zhang and B. A. Wandell, "A spatial extension of CIELAB for digital color-image reproduction," *Journal of the Society for Information Display*, vol. 5, no. 1, pp. 61–63, 1997.

[27] M. R. Luo, G. Cui, and B. Rigg, "The development of the CIE 2000 colour-difference formula: CIEDE2000," vol. 26, no. 5, pp. 340–350, Oct. 2001.

[28] G. Sharma, W. Wu, and E. N. Dalal, "The CIEDE2000 color-difference formula: Implementation notes, supplementary test data, and mathematical observations," *Color Res. Appl.*, vol. 30, no. 1, pp. 21–30, Feb. 2005.

[29] CIE, "Colorimetry," CIE Publication No. 15.2, Central Bureau of the CIE, Vienna, 1986.

[30] G. Sharma and C. E. Rodríguez-Pardo, "The dark side of CIELAB." in *Proc. SPIE: Color Imaging XVII: Displaying, Processing, Hardcopy, and Applications*, vol. 8292, 2012, pp. 8292–0D,1–10.

[31] B. Schauerte and R. Stiefelhagen, "Quaternion-based spectral saliency detection for eye fixation prediction," *Computer Vision–ECCV 2012*, pp. 116–129, 2012.

[32] K. Dinesh and G. Sharma, "Per-channel color barcodes for displays," in *IEEE Intl. Conf. on Image Proc. (ICIP), 2016*. IEEE, 2016, pp. 3992–3996.

Author Biography

Karthik Dinesh received B.E in Electronics and Communication from National Institute of Engineering, Mysore, India and M.Tech from Indian Institute of Technology, Kanpur, India. He is currently pursuing PhD in ECE department, University of Rochester under the supervision of Dr. Gaurav Sharma.

Gaurav Sharma is a professor at the University of Rochester in the Department of Electrical and Computer Engineering, in the Department of Computer Science, and in the Department of Biostatistics and Computational Biology. He is the editor of the Color Imaging Handbook, published by CRC Press in 2003. He is a fellow of the Society of Imaging Science and Technology (IS&T), of SPIE, and of the IEEE, and a member of Sigma Xi.